Space debris removal by non-destructive orbit modification using ground-based high-power lasers

Stefan Scharring[(1)] and Jürgen Kästel[(2)]

[(1)] German Aerospace Center (DLR), Institute of Technical Physics, Pfaffenwaldring 38 – 40, 70569 Stuttgart, Germany; stefan.scharring@dlr.de
[(2)] German Aerospace Center (DLR), Institute of Technical Physics, Pfaffenwaldring 38 – 40, 70569 Stuttgart, Germany; juergen.kaestel@dlr.de

Abstract

Accelerated deterioration of ecosystems naturally expands situational awareness from sustainability efforts towards emergency response. While this holds true for, e.g., climate change, the current evolution of Earth's orbital environment develops into a status demanding for short-term action far beyond sustainability measures for space debris mitigation. Possibly not being the most relevant option for space sustainability efforts, high-power lasers might nonetheless play a significant role in response to the increasing number of known debris objects. Lasers, however, with a perception ranging from well-known everyday life applications via technology optimism and weaponization efforts up to visionary propulsion concepts, demand for a thoughtful assessment of their beneficial as well as their destructive potential regarding thermo-mechanical interaction with space debris.

In our work we present a holistic approach to realistically assess conceivable contributions of ground-based high-power laser technology for mitigation of the space debris situation in the low Earth orbit. Departing from experimental work on laser-induced momentum coupling, our simulations cover aspects of beam transmission like atmospheric extinction, turbulence compensation, and beam pointing jitter. Laser-matter interaction is computed considering different generic target shapes, various target materials as well as the dependency of thermo-mechanical coupling on the incident laser fluence. Moreover, estimates are derived on the debris remediation performance of a repetitive 100 kJ laser system for perigee lowering to achieve atmospheric burnup after multiple laser station overpasses. The related laser irradiation constraints for operational safety are explored in terms of the target's thermo-mechanical integrity throughout the entire orbit modification maneuver.

1 INTRODUCTION

In the past decades, the increasing congestion of the low Earth orbit (LEO) by space debris has frequently been perceived as a disaster in slow motion with a threatening perspective of future exponential increase and runaway effect, the so-called Kessler syndrome [1], but still with time left to act in a sustainable way by debris avoidance regulations, timely post-mission disposal and eventually pursuing active debris removal (ADR) of at least 5 large debris objects per year [2]. While such large objects have already been prioritized [3] and first attempts to actively remove debris objects are on their way of technological implementation [4,5], a possible onset of the Kessler syndrome in the highly frequented LEO altitudes has been reported recently [6]. Correspondingly, a survey about debris remediation technologies [7] has been issued by the U.S. National Aeronautics and Space Administration (NASA) that focuses rather on economic aspects than prioritizing sustainability issues. In that analysis of ADR costs and benefits, removal of multiple small debris fragments and collision avoidance for large objects are recommended as the most-effective methods to reduce risks to space operators.

The concept of de-orbiting small sized space debris remotely using high energy lasers on ground has firstly been elaborated in the ORION study in the 1990's [8]. While development risks, system complexity, safety requirements and financing needs are challenging, the perspective of debris removal without the need for a dedicated space mission is certainly compelling and gave rise to several similar studies [9,10] including related work envisaging a space-based laser [11] or even hybrid concepts [12]. All these concepts are based on laser-induced surface ablation which yields momentum imparted to the debris from the recoil of the ablation jet. Focused, high intensity laser pulses are required, typically several Joules of laser pulse energy per cm² target area, delivered during a laser pulse duration of only a few tens of nanoseconds. Momentum transfer can be very effective, up to 1 mN per Watt average laser power, but the heat that is deposited into the target during the ablation process can severely accumulate during a long series of high energy laser pulses, eventually endangering the target's mechanical integrity [13]. Since the object's premature disintegration long before its final de-orbit might even aggravate the space debris situation, thermal constraints have to be carefully observed in order not to overestimate the performance of a laser-based system for space debris removal.

2 METHOD

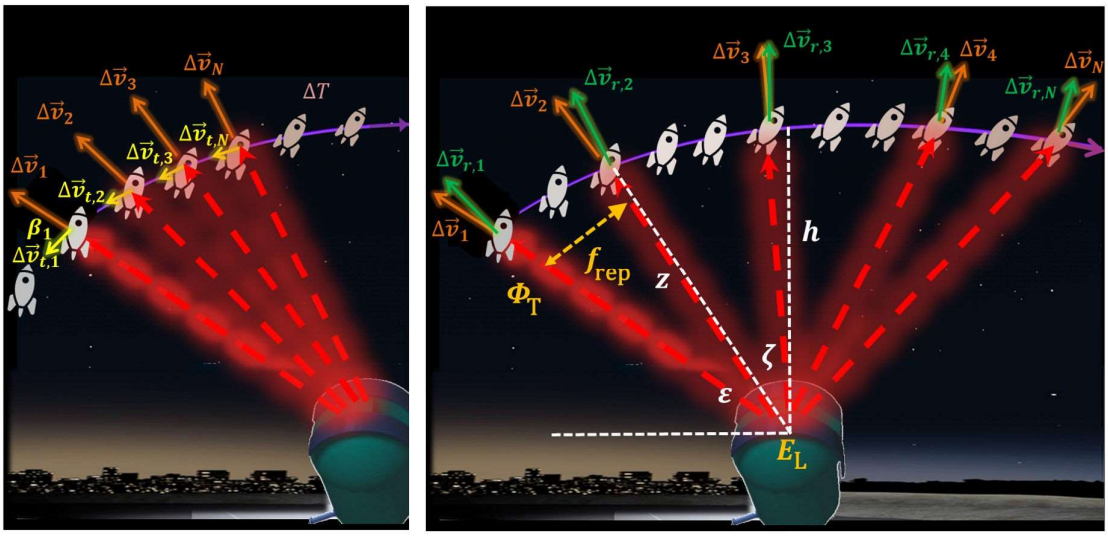

(a) (b)

Fig. 1. Schematics of different ground-based irradiation scenarios for laser-induced orbit modification: (a) Head-on irradiation for in-track deceleration and (b) outward irradiation momentum for apogee lift. Both methods can be used for perigee lowering of space debris to eventually initialize the object's de-orbit by atmospheric drag if applied during multiple station transits. Figure taken from [14] under Creative Commons license CC-BY 4.0.

In our study, which is outlined in greater detail in [14], we analyze the perigee lowering of different space debris objects that can be achieved by recoil from laser-induced surface ablation during a direct overpass over a ground station with a repetitively pulsed high energy laser, cf. Fig. 1. For this purpose, the transmitted laser fluence Φ_T is computed from laser and transmitter specifications taking account of atmospheric extinction and turbulence compensation. From this, the velocity changes Δv_i can be computed for each one of the N laser pulses from the momentum coupling coefficient $c_m = m\Delta v/E$

where m is the debris mass and E is the incident laser pulse energy. Moreover, the temperature rise ΔT due to the amount of laser-deposited heat $Q = \eta_{res} \cdot E$ is derived from the residual heat coefficient η_{res}, which allows to monitor target-specific limitations and maintain its thermo-mechanical integrity. Finally, the change of perigee is obtained from the overall amount of radial and in-track velocity change Δv_r and Δv_i, respectively.

The 1111 space debris objects in LEO which are considered in our study comprise high risk objects like ENVISAT and SL-16 rocket bodies prioritized in [3] for ADR regarding space sustainability as well as medium-sized payloads, fragments from anti-satellite weapon tests (ASAT) and other fragments from explosions and collisions of payloads and rocket bodies, see Tab. 1 for details.

Tab. 1. Simulation targets for laser-matter interaction in debris removal: In the raytracing simulations objects are represented by geometric primitives. For thermo-mechanical coupling, data for aluminum and steel, cf. Fig. 2, has been assigned depending on the debris' origin (payload or rocket body, resp.). Debris data have been obtained with permission from [15].

	Number	Size $L_c\ [m]$	Mass $m\ [kg]$	Material	Simplified shape(s)
High-risk satellite	1	11.5	8110	aluminum	cuboid
High-risk rocket bodies	10	3.6–8.7	1190–9000	steel	cylinder, ellipsoid
Medium-sized payloads	100	0.5–5.5	50–991	aluminum	sphere, cuboid, cylinder
Payload fragments	371	0.11–0.33	1.1–29.2	aluminum	flake
ASAT fragments	342	0.11–0.30	1.1–22.9	aluminum	flake
Rocket body fragments	287	0.11–0.36	1.1–37.3	steel	flake

2.1 Laser power beaming from ground to orbit

A repetitively pulsed laser system with an overall pulse energy of $E_L = 100\ kJ$ is anticipated as remote ground-based energy source for orbit modification. The system architecture is based on coherent coupling of 5000 single laser emitters with 20 J pulse energy each, operating at $\lambda = 1030\ nm$ wavelength and $\tau = 5\ ns$ pulse length with a superior beam quality of $M^2 = 1.5$, cf. our recent developments lined out in [16].

Laser power beaming from a large-aperture telescope to space debris in LEO demands not only continuous tracking of the debris object during its overpass but it also requires to employ laser ranging in order to use real-time data to adjust the transmitter's focal length to its rapidly changing distance z from the target. Regarding telescope pointing we assume a tracking data uncertainty of $\sigma_t = 0.1"$ [17] while the performance of tip-tilt correction of beam pointing is assessed following [18] with a pointing jitter of $\sigma_p = 0.17"$ at zenith up to $\sigma_p = 0.63"$ at a zenith angle of $\zeta = 65°$.

For beam transmission, a laser guide star is employed pointing slightly ahead the debris position to probe optical wavefront distortion due to atmospheric turbulence. The related signal, detected with a Shack-Hartmann sensor on ground, is then used to dynamically adapt the phase shift of the single laser emitters to imprint a complementary pre-deformation to the emitted laser beam. This allows to strongly limit the impact of turbulence-induced beam broadening on the focus spot diameter d_s in orbit, which can be derived from

$$d_s = \frac{M^2 \lambda\, z}{0.56\, D_T \sqrt{Str}} \tag{1}$$

where $D_T = 4\ m$ is the aperture diameter of the transmitter and Str is its Strehl ratio. The latter is mainly determined by the response frequency and spatial configuration of the phase correction system and ranges from 0.16 to 0.35 in our case, dependent on target altitude h and elevation ε.

From transmitter system considerations on the tiled aperture concept, we estimate the far-field power-in-the-bucket discarding side lobes to be around $S_{PIB} \approx 65\ \%$ of the transmitted laser pulse energy. For atmospheric extinction, the database for clean air at $\lambda = 1.06\ \mu m$ from [19] has been used reporting a transmissivity of $T = 71.1\ \%$ at $\zeta = 65°$ up to $T = 86.6\ \%$ at zenith. Thus, the transmitted laser pulse energy is given by $E_T = S_{PIB} \cdot T \cdot E_L$ and the average fluence at the debris position can be derived as $\langle \Phi_T \rangle = E_T / A_s$ where $A_s = \pi\, d_s^2 / 4$ is the laser spot area.

2.2 Laser-matter interaction for orbit modification

The laser fluence is a crucial parameter to assess the magnitude of imparted momentum and heat deposition in laser ablation which both depend non-linearly on the fluence, cf. Fig. 2. Note that for laser ablation a certain threshold fluence Φ_0 has to be exceeded while heat deposition is already present for fluences below Φ_0.

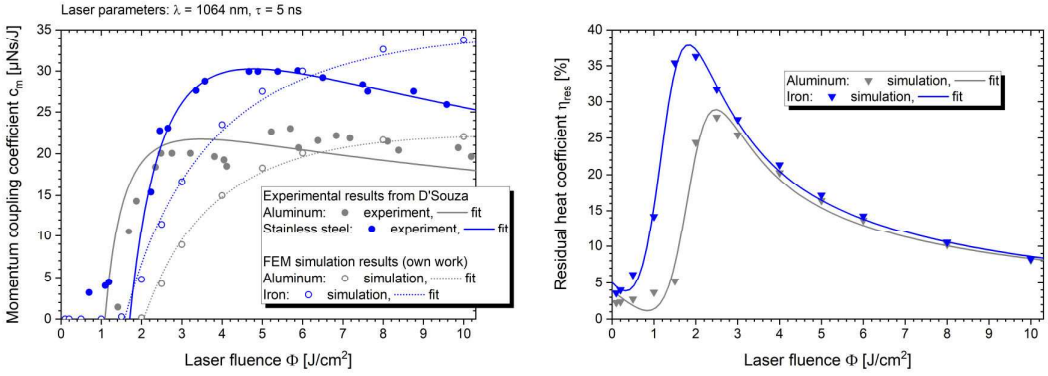

(a) (b)

Fig. 2. FEM simulation results for (a) laser-induced momentum and (b) deposited heat, resp., per laser pulse energy at $\lambda = 1064\ nm$ and $\tau = 5\ ns$. For momentum coupling, simulation results for different laser fluences are compared with experimental data from [20]. Figure taken from [14] under CC-BY 4.0.

In our analysis, the pulsed laser operates at a repetition rate f_{rep} during a certain elevation range of the overpass, see below. Within this interval, the laser fluence is computed for each laser pulse allowing to derive the temperature increase from the coefficient of residual heat. While the average fluence is used to assess heat coupling, a more sophisticated approach is employed to analyze the laser-imparted momentum. For that purpose, our raytracing-based algorithm EXPEDIT [13] is used which allows for a discretized analysis of the various contributions to laser-ablative momentum imparted to the different surface elements of the target which are hit by the different rays of the laser beam considering their individual fluence within the Gaussian beam profile.

Laser-ablative momentum is derived with EXPEDIT for each target at its mean orbit altitude for twelve different zenith angles from $\zeta = 0°$ up to 65° in steps of $\Delta\zeta = 5°$ and interpolated for elevations in between. Beam pointing jitter and the missing information about target orientation are incorporated into the simulations using a Monte Carlo approach introducing a randomly sampled beam center offset from the target's center of mass, with a Gaussian distribution that corresponds to the beam pointing jitter, and a random orientation for each simulation sample, which finally gives an averaged imparted momentum of which the component aligned co-axially with the beam direction is used to assess orbit modification, cf. Fig. *1*.

From the laser-induced in-track and radial velocity change after a station pass, Δv_t and Δv_r, resp., the change of perigee altitude Δh_p can be computed [12] using

$$\Delta h_p = (1 - e_0)\Delta a - (a_0 + \Delta a)\Delta \mathrm{e} \tag{2}$$

where the change of orbit eccentricity Δe and semi-major axis Δa are given by

$$\Delta e = [2(e_0 + \cos\varphi_0)\Delta v_t - r_0 \sin\varphi_0 \cdot \Delta v_r / a_0]/v_0 \text{ and} \tag{3}$$

$$\Delta a = 2a_0^2 v_0 \Delta v_t / GM, \tag{4}$$

a, e, r, φ are semi-major axis, numerical eccentricity, orbit radius and true anomaly, respectively, $GM = 398600.4\, km^3/s^2$ is Earth's gravitational constant, and the subscript 0 indicates the orbital parameters before the station pass. As a simplification, we combine the laser-induced velocity changes from the different pulses to a single Δv by adding up the magnitudes of each vector component discarding the changing beam orientation throughout the encounter. Instead, an instantaneous velocity change is assumed, for which we selected a true anomaly of $\varphi_0 = 270°$.

3 RESULTS

For each object class we derived an altitude-dependent optimized elevation range in which irradiation should be undertaken. In the case of head-on irradiation there is a trade-off between a relatively large in-track component of the imparted momentum for low elevation angles while at high elevation angles, we have high laser fluences and small outshining losses. Hence, the in-track component of laser-imparted momentum has been analyzed as function of the zenith angle. The results can be approximated by a Gaussian fit from which the full width at half maximum (FWHM) has been taken as irradiation interval defining the zenith angles ζ_{in} and ζ_{out} for start and stop of laser irradiation, respectively. Likewise, the imparted radial momentum has been analyzed for the case of outward irradiation yielding a Gaussian fit centered at zenith, i.e., $\zeta_{out} = -\zeta_{in}$ while head-on irradiation is limited to the ascending part of the station transit.

Within the specified elevation range laser irradiation of debris fragments at 100 Hz pulse repetition rate has been analyzed. We found that the laser-induced temperature increment, which can be deduced from the definition of the residual heat coefficient via $\Delta T \approx (A/m)\left(1/c_p\right)\sum_{i=1}^{N} \eta_i(\Phi_i) \cdot \Phi_i$ (where Φ_i is the fluence at the target from the ith pulse), would exceed the melting point of a large number of fragments with a high area-to-mass ratio. Melting, however, could result, e.g., in splashing during laser ablation or in sphere formation and subsequent loss of trackability. Therefore, the pulse repetition rate

has been constrained to 9 Hz for head-on irradiation and 6 Hz for outward irradiation. Thus, the temperature increase due to laser heat deposition is limited to 100 K for aluminum and 200 K for stainless steel which is approximately 20% of the increase from 0°C up to the melting point for fragments with high A/m. Under these constraints, the overall velocity change after laser irradiation is in the order of a few m/s, cf. Fig. 3, about two orders of magnitude below the Δv required for de-orbit. Hence, a multitude of laser station transits with interim target cooldown would be required for perigee lowering that eventually yields in de-orbit by atmospheric drag.

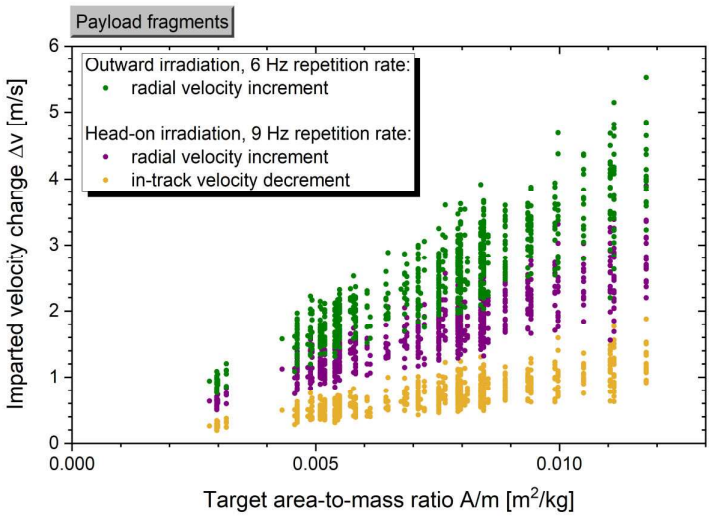

Fig. 3. Simulation results for the velocity change of space debris after laser irradiation during a station overpass. Figure taken from [14] under CC-BY 4.0.

While only bulk material properties were considered for the thermal constraints of fragments, complex targets like defunct satellites or spent upper stages demand for a separate treatment regarding their thermo-mechanical integrity. Here, we referred to [21] where the lethality threshold for thermal kill of unhardened satellites was stated to be significantly below 100 W/cm². Hence, a maximum intensity of 13.7 W/cm² (hundredfold of the solar constant) has been chosen to constrain outward irradiation whereas 20.6 W/cm² was the upper limit for head-on irradiation. In turn, repetition rates were in the range of 1.1 to 3.8 Hz and 1.6 to 5.7 Hz, respectively, dependent on the debris altitude.

For the specified elevation ranges and pulse repetition rates, the changes of orbital velocity after a station overpass have been computed for all 1111 targets. Regarding the related outcome of the laser maneuver in terms of perigee lowering we surprisingly found that ground-based, i.e., oblique pointing, head-on irradiation outperforms outward irradiation by approximately 23 ± 8 %, indicating that, unlike for a Hohmann transfer with $\varphi_0 = 180°$, not only in-track deceleration contributes in head-on irradiation if a suitable true anomaly is selected for irradiation, cf. Eq. 3.

The summary of the results on perigee lowering in Fig. 4 shows that successful de-orbiting demands for laser irradiation during multiple station transits since perigee lowering only amounts to a few kilometers for fragments. Extrapolating the results for fragments we find that on average 240 ± 130 station overpasses with laser irradiation are required to eventually lower the perigee altitude down to 200 km. For payloads more than 1000 passes are typically required, in particular when their size exceeds 2 m, while for the high-risk targets, between 3000 and 30,000 irradiations would be needed for de-orbit.

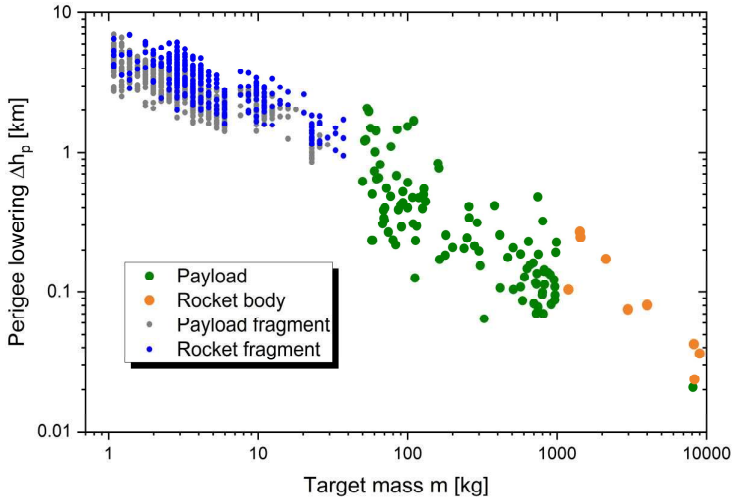

Fig. 4 Perigee lowering after ground-based head-on laser irradiation: Simulations results from ray-tracing based momentum computation for 1111 different space debris targets in the low Earth orbit. Laser parameters: 100 kJ pulse energy, 5 ns pulse length, 1030 nm wavelength. Transmitter aperture: 4 meters, turbulence compensation with adaptive optics, tracking uncertainty: 0.1 arcsecs. Debris irradiation interval and pulse repetition rate: target-specific, see text. Figure from [14] under CC-BY 4.0.

4 DISCUSSION

The study's findings on achievable perigee lowering from a single station overpass might appear disappointing at a first glance, in particular when having in mind that earlier studies on laser-based removal of space debris had been significantly more promising, cf. the related number of passes for re-entry and the removal efficiencies shown in Tab. 2. The reasons for these discrepancies can be attributed to the different assumptions employed in the simulations.

4.1 Ground station

Comparing the laser specifications of the different studies, the high laser pulse energy specified in our study is rather striking, cf. Tab. 2. One of the main reasons for this energy selection can be found in our choice to limit the transmitter's aperture to max. 4 m which enables the usage of a single laser guide star for beam pointing. In turn, cf. Eq. 1, a larger laser spot in orbit demands for a higher laser pulse energy in order to achieve the required fluence for efficient momentum coupling. Moreover, our computations on near-term available adaptive optics for this transmitter configuration yield a comparably low Strehl ratio which again contributes to the comparatively large laser spot size.

Another main point is the hit uncertainty of the laser beam. While, to our knowledge, the impact of pointing jitter and tracking uncertainty on the laser-imparted momentum has been discarded in the mentioned earlier studies, we explicitly included this by introducing an arbitrary offset in the Monte Carlo studies for momentum computation in our work. Using the hit uncertainty $\sigma_h = \sqrt{\sigma_t^2 + \sigma_p^2}$ as the source of randomness in beam offset computation, the impact of having in average 0.3 ± 0.13 arcsecs uncertainty should yield a decrease of imparted momentum by a factor of at least 5, as shown in [17], albeit for photon pressure. Therefore, it appears reasonable to partially compensate for this performance loss by the selection of a relatively high laser pulse energy.

Tab. 2 Parameter comparison for studies on laser-based debris removal from LEO [8,9,10,14,22,23]. Numbers printed in bold indicate different data and results for the case of large, not fragmented debris.

	ORION	LODR	CLEANSPACE	This study
Study year	1996	2012	2014	2023
Pulse energy [kJ]	20	7.3 (**140**)	20	100
Wavelength [µm]	0.53	1.06	approx. 1	1.03
Pulse length [ns]	40	5 (**10**)	5	5
Beam quality parameter M^2 [-]	2.5	2	< 2.5	1.5
Pulse repetition rate [Hz]	1	11.2	50	9 (**1.6 – 5.7**)
Transmitter aperture [m]	6	13(**25**)	6	4
Strehl ratio [-]	0.5	0.25	> 0.4	0.16 - 0.35
Orbit range [km]	below 1000	below 700 (**900**)	585 and 688	579 - 1179
Debris mass [kg]	0.0001 - 100	max. 0.75 (**1000**)	n.d.	1 - 50 (**50 - 10,000**)
Debris size [m]	0.01 - 1	max. 0.31 (**1.25**)	max. 0.1	0.11 - 0.36 (**0.5 - 11.5**)
Area-to-mass ratio [m^2/kg]	0.0079 - 0.79	0.1 (**0.0012**)	0.11 and 0.28	0.0025 - 0.012 (**0.0018 - 0.15**)
Number of passes for re-entry	1 (1cm, 0.1 g) 12 (10cm, 100g) 780 (1m, 100kg)	1 (**135**)	10 - 15	100 - 400 (**200 - 30,000**)
Removal efficiency [objects/year]	50,000	140,000 (**450**)	n.d.	2000 (**n.d.**)

4.2 Laser-induced Momentum and Heat

In our recent study and in the CLEANSPACE project, momentum coupling coefficients of up to 30 µNs/J [23] have been assumed considering their non-linear dependency on the laser fluence. In ORION and LODR, however, a significantly higher value for c_m has been employed (100 µNs/J and 75 µNs/J, respectively) as a constant value, which, looking at the experimental database of our study, appears to be too optimistic and yields a removal performance which is likely overestimated by a factor of 2 to 5.

Thermal constraints due to possible target melting have not been considered in the earlier studies reviewed here. However, target heating of debris fragments can easily be estimated for those studies using $\Delta T = Q/(c_p \cdot m) \approx (\eta_{res} \cdot \Phi_T \cdot f_{rep} \cdot t_L)/c_p \cdot A/m$ where t_L is the time interval of irradiation during the transit. Assuming $\eta_{res} \approx 0.1$ and $c_p \approx 900\ J/(kg \cdot K)$ using the configurations given above we find that in the ORION study our requirement of $\Delta T \leq 100\ K$ would be fulfilled for debris larger than 5 cm. However, the laser-induced temperature increase exceeds this constraint by one (LODR) up to more than two (CLEANSPACE) orders of magnitude, which in turn results in a significant underestimation of the number of passes required for de-orbit. Regarding the thermo-mechanical stability of large

targets, we find that the mean intensity of 20.3 W/cm² employed in the LODR study is in good agreement with our irradiation limits.

5 SUMMARY

In comparison to earlier studies on removal of space debris using ground-based lasers we have found that the selection of a relatively small (4 meters) transmitter architecture together with a notable tracking and pointing uncertainty (0.3 arcsecs) demands for a high laser pulse energy (100 kJ) which exceeds the specifications from previous work on ADR of fragments by around one order of magnitude. Consideration of experimental data on momentum coupling for a broad range of fluences suggests that the laser-imparted momentum is by a factor of 2 to 5 lower than predicted in those earlier studies where Δv had been computed from c_m data which seem to constitute rather optimistic values and, moreover, discard the dependency of c_m on the fluence.

As a novel approach in the conceptual research on laser-based space debris removal we have introduced irradiation limits for the average intensity and/or the maximum laser pulse number based on thermal constraints which would have easily been exceeded in some earlier studies. Therefore, the system performance in debris removal predicted in our study is not only significantly lower than assessed elsewhere but this finding also points to a possibly very smooth transition from laser-based orbit modification to laser-based weaponization.

Given all these constraints, the predicted efficiency of using ground-based lasers to de-orbit the top priority debris objects for sustainability in LEO is too low not to put its reasonability into question. From the economical viewpoint, however, cf. [7], regarding the increasing burden for collision avoidance that comes with the escalating number and the rising awareness of small-sized space debris, such laser systems could support future space operations very well due by ADR of a multitude of small objects – even if the impact of laser-based removal on space sustainability itself might still remain marginal.

6 ACKNOWLEDGMENTS

The authors gratefully acknowledge the DLR team contributions from Wolfgang Riede and Jochen Speiser in funding acquisition and study supervision, from Jascha Wilken, Lukas Eisert and Erik Klein in software development, and from Samantha Rose Siegert in language editing of the manuscript. Furthermore, we give thanks to ESA for data usage from DISCOS and Master-8 and to USSTRATCOM for making TLE data accessible. The debris simulation target catalog has been taken with permission from our recent study LARAMOTIONS [17] under ESA contract 4000127148/19/D/CT. Here, we express our thanks in particular to Christoph Bamann, formerly at TU Munich, Germany, now at Vyoma GmbH, for the compilation of mass and optical cross-section for debris fragments from the Master-8 statistics.

7 REFERENCES

1. Kessler, D.J. and Cour-Palais, B.G. Collision Frequency of Artificial Satellites: The Creation of a Debris Belt, *Journal of Geophysical Research*, vol. 83, pp. 2637-2646, 1978.
2. Liou, J.-C. An active debris removal parametric study for LEO environment remediation, *Advances in Space Research,* vol. 47, pp. 1865-1876, 2011.
3. McKnight, D., *et al.* Identifying the 50 statistically-most-concerning derelict objects in LEO, *Acta Astronautica*, vol. 181, pp. 282-291, 2021.
4. Clearspace-1. Available at https://www.esa.int/Space_Safety/ClearSpace-1, accessed 17 March

2023.

5. Astroscale. Available at https://astroscale.com/astroscale-selects-rocket-lab-to-launch-phase-i-of-jaxas-debris-removal-demonstration-project/, accessed 17 March 2023.
6. Phipps, C. and Bonnal, C. Laser Ranging and Nudging in Space Debris Traffic Management, *Sensors & Transducers Journal*, vol. 255, 17-23, 2022.
7. Colvin, T.J., Karcz, J., and Wusk, G. "Cost and Benefit Analysis of Orbital Debris Remediation," NASA Office of Technology, Policy, and Strategy, Washington D.C., 2023.
8. Phipps, C.R., *et al.* ORION: Clearing near-Earth space debris using a 20-kW, 530-nm, Earth-based, repetitively pulsed laser, *Laser and Particle Beams*, vol. 14, no. 1, pp. 1-44, 1996.
9. Phipps, C.R., *et al.* Removing orbital debris with lasers, *Advances in Space Research*, vol. 49, pp. 1283-1300, 2012.
10. Esmiller, B., *et al.* Space debris removal by ground-based lasers - Main conclusions of the European project CLEANSPACE, in: T. Sgobba and I. Rongier (eds.), *Space Safety is No Accident*, Springer, 2015.
11. Soulard, R., *et al.* ICAN: A novel laser architecture for space debris removal, *Acta Astronautica*, vol. 105, 192-200, 2014.
12. Wen, Q., et al. Removing small scale space debris by using a hybrid ground and space based laser system. *Optik*, vol. 141, pp. 105-113, 2017.
13. Scharring, S., et al. Momentum predictability and heat accumulation in laser-based space debris removal, *Optical Engineering*, vol. 58, no. 1, 011004 (2019)
14. Scharring, S. and Kästel, J. Can the Orbital Debris Disease Be Cured Using Lasers? *Aerospace*, vol. 10, article 633, 20 pages, 2023.
15. DISCOS Database, Space Debris User Portal, European Space Agency-European Space Operations Center (ESA/ESOC). Available at https://sdup.esoc.esa.int/, accessed on 2 July 2019.
16. Speiser, J., et al. "Thin Disk Laser Development for Space Debris Monitoring and Mitigation," in: Proceedings of the 2022 Conference on Lasers and Electro-Optics (CLEO), San Jose, CA, USA.
17. Scharring, S., *et al.* LARAMOTIONS: a conceptual study on laser networks for near-term collision avoidance for space debris in the low Earth orbit, *Applied Optics*, vol. 60, no. 31, pp. H24-H36, 2021.
18. Olivier, S.S. and Gavel, D.R. Tip-tilt compensation for astronomical imaging. *Journal of the Optical Society of America A*, vol. 11, pp. 368-378, 1994.
19. McClatchey, R.A., *et al*. "Optical Properties of the Atmosphere," Air Force Cambridge Research Laboratories, Bedford, MA, USA, 1972.
20. D'Souza, B.C. "Development of Impulse Measurement Techniques for the Investigation of Transient Forces due to Laser-Induced Ablation," Ph.D. Thesis, Los Angeles, CA, USA, 2007.
21. Bloembergen, N., *et al.* Beam Material Interactions and Lethality, *Reviews of Modern Physics*, vol. 59, no. 3, part II, pp. S119-S143, 1987.
22. Wnuk, E., *et al.* Future Orbits of Space Debris after LDR Operation, Proc. 6th European Conference on Space Debris, ESA, SDC6 paper 131, 2013.
23. Eckel, H.-A., Göge, D., and Zimper, D. Laser-Based Space Debris Removal – An Approach for Protecting the Critical Infrastructure Space, *Journal of the JAPCC*, vol. 22, pp. 75-84, 2016.